

Potential Flow Solutions with Wakes over an Ogive Cylinder

Ismail H. Tuncer* and Max F. Platzer†

U.S. Naval Postgraduate School, Monterey, California 93943

An incompressible panel code is employed to compute the flow over an ogive cylinder body with an overall length of 7.5 diameter. Flow separation is modeled by vortex wakes attached to the base region and the leeward sides of the cylinder body. The computed surface pressures and integrated normal force and pitching-moment coefficients are found to be in good agreement with the experimental data up to 20-deg incidence. This favorable agreement suggests that the panel codes may be a computationally efficient tool in the aerodynamic missile design process at low incidences.

Nomenclature

D	= diameter of ogive cylinder body
L	= length of ogive cylinder, $7.5D$
L_N	= nose fineness, $3.5D$
Re_D	= Reynolds number based on diameter
t	= time, nondimensional
x/D	= axial position
α	= incidence angle, deg
Δt	= time-step size for wakes, nondimensional
Θ	= circumferential position, deg
Θ_w	= circumferential position of wake separation line, deg

Introduction

It is recognized that computational fluid dynamics tools are becoming practical in the prediction of missile aerodynamics. The recent advances in the aerodynamic prediction methodology for tactical missiles have been documented.¹ Rom² also presents the current aerodynamic analysis methods and numerical calculations for high-angle-of-attack flows. The current aerodynamic prediction methods range from semiempirical methods, such as AP-95 (Ref. 3), to panel methods and complete Euler and Navier–Stokes computations. Each method has its own set of advantages and limitations, and much more work is required to fully understand the merits and applicability of these methods. Therefore, for the time being, it appears advisable to retain all of the methods in the missile aerodynamicist's tool kit.

Most of the previous work in prediction of missile aerodynamics was devoted to simpler configurations, especially to bodies of revolution.^{4–8} Lately, Navier–Stokes solutions also have been obtained for full missile configurations.^{9–11} However, current air-to-air missile aerodynamic design work is done primarily using prediction codes based on semiempirical methods. These tools are limited to previously investigated missile configurations and flight regimes. Panel codes are therefore the next logical step in refining these tools because of their relative robustness and computational efficiency and because they allow for any arbitrary configuration to be modeled inexpensively within the limitations of inviscid aerodynamics. Inviscid panel codes with simulated wakes can be expected to yield accurate results for low-speed flows at a significantly reduced computational cost.

It is the objective of the present study to employ the panel code PMARC (Panel Method Ames Research Center), developed by the NASA Ames Research Center, for the simulation of separated flows over an ogive cylinder (Fig. 1) at high incidences and to evaluate the suitability of panel codes for aerodynamic missile design work. Recently, Lambert and Platzer¹² evaluated the PMARC code by

favorably comparing its predictions with various experimental data. Tuncer et al.¹³ also employed PMARC for flows over a missile forebody at low angles of attack.

PMARC: Potential Flow Solver

PMARC is a low-order potential flow solver for simulating flows over complex three-dimensional geometries. The flowfield is assumed to be inviscid, irrotational, and incompressible. PMARC solves the Laplace equation for the velocity potential over a closed body using doublets and source singularities placed on solid surfaces and wakes. The singularities are distributed with constant strength over each panel, which makes PMARC a low-order panel method, in contrast to higher-order methods where singularity strengths are allowed to vary linearly or quadratically over each panel. Unknown doublet and source strengths are determined by imposing the proper flow tangency and trailing-edge conditions. The linear system of equations then is solved using an iterative matrix solver. Once the unknown doublet and source strengths are determined, tangential velocity components and pressure coefficients on each panel are evaluated. Further details of the PMARC code can be found in Ref. 14. In this study, we used the latest PMARC version, 12.22.

In PMARC, wakes can be shed from trailing edges of lifting surfaces or from prescribed separation lines along the panel distribution. The wakes are convected downstream by marching in time. The first row of wake panels is shed from the separation line at time $t = 0$. With each subsequent time step, a new row of wake panels is added to the wake at the separation line, and all of the preceding rows of wake panels are convected downstream. The Kutta condition, which states that there is no pressure discontinuity at the stagnation point, is used to determine doublet strengths on the first row of wake panels. Wake-panel trajectories may be rigid or flexible. Rigid wakes are convected with the freestream velocity, whereas flexible wakes are convected with the local flow velocity at each time step. Although the flexible wakes are more realistic, in this study we employed rigid wakes due to the strong interaction between the flexible wakes shed from the base corner and from the body and the resulting divergence of the solution.

PMARC has an option for modeling symmetric flowfields. With this option activated, the model is only paneled in half, and symmetrical influence coefficients account for the other symmetrical half in the lateral direction. In the present study the flowfield is assumed to be symmetric, and only the half ogive cylinder body is paneled. Thus, only the symmetric wakes are considered.

It also was observed that the computed source strengths at the base region exhibit an oscillatory behavior along the time steps, which causes the time rate of change of velocity potential, $\partial\phi/\partial t$, to attain unrealistic values. Because a steady solution is sought as the time stepping proceeds, the contribution to the surface pressure from the $\partial\phi/\partial t$ term is neglected in the present computations.

Results and Discussion

In this study, a series of flowfields over the tangent ogive cylinder body with a nose fineness ratio of $L_N/D = 3.5$ and with an overall

Received May 7, 1997; revision received Nov. 29, 1997; accepted for publication Dec. 11, 1997. This paper is declared a work of the U.S. Government and is not subject to copyright protection in the United States.

*Research Assistant Professor, Department of Aeronautics and Astronautics, Member AIAA.

†Professor, Department of Aeronautics and Astronautics, Associate Fellow AIAA.

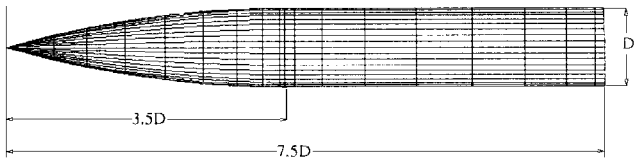


Fig. 1 Ogive cylinder body.

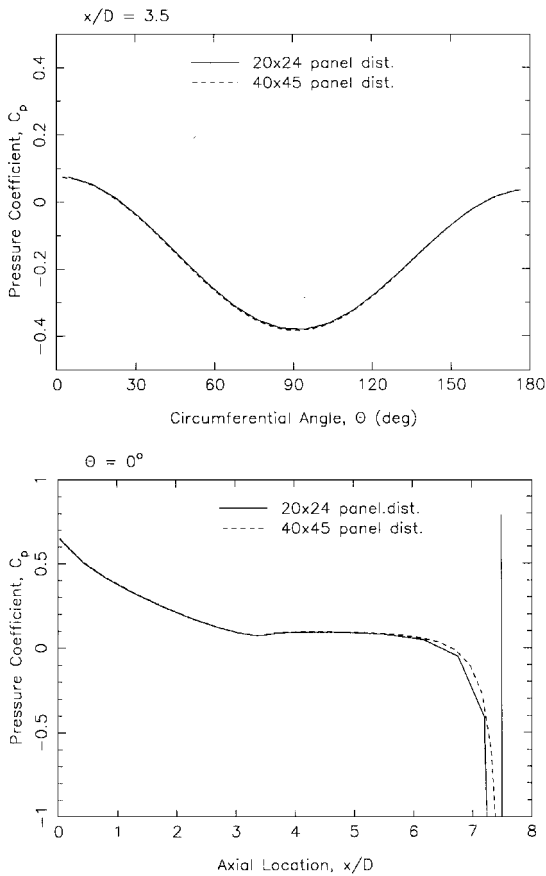


Fig. 2 Sensitivity of surface pressure distribution to surface panel distribution at $\alpha = 20$ deg.

length of $L/D = 7.5$ was investigated. After an initial panel distribution sensitivity study for the steady-state solution at $\alpha = 20$ deg (Fig. 2), the symmetric half-body was paneled with a total of 480 (20×24) panels throughout all of the computations. Twenty panels were distributed equally along the circumferential direction. Nineteen panels were placed along the axial direction with a cosine distribution over the ogive and the cylindrical sections as shown in Fig. 1. Five panels were distributed similarly in the radial direction at the base section of the cylinder. The recommended convergence criterion of 0.0005 was used for the iterative solution at each time step. In the computations, we employed two wakes: one shed from the base corner and the other shed along the cylindrical body. The circumferential position of the wake separation line along the cylindrical body was varied parametrically, whereas the axial starting position was fixed on the basis of experimental data. All computations were performed on workstations. CPU requirements were on the order of 10 min, depending on the number of time steps. In the present computations, one of the three influence coefficient matrices is stored in memory, which is the only allowed compile time option. Note that, because the other coefficient matrices stored on disk are read in line by line for each time step, fast disk access and I/O buffering improve the total run time considerably.

We first computed the flowfield at $\alpha = 20$ deg by attaching just a single wake from the base corner. Figure 3 shows the influence of the base wake on the surface pressure distribution as a function of time-step size. The solutions were obtained by marching in time with a fixed time step, Δt , until a converged steady-state solution was

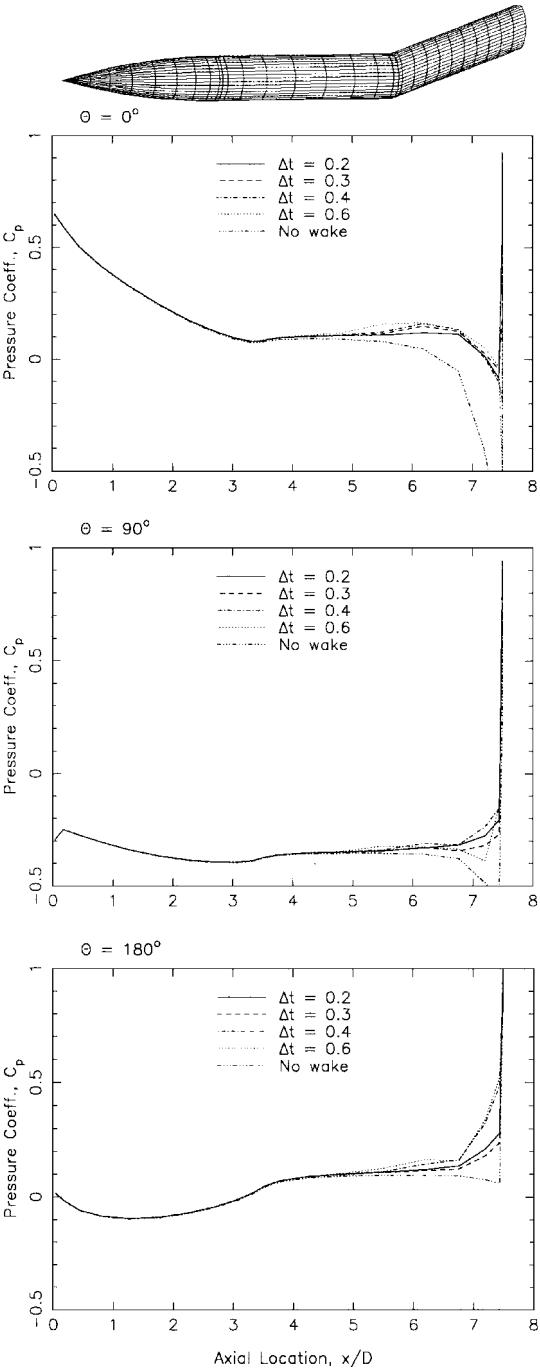


Fig. 3 Influence of base corner wake on surface pressure distribution at $\alpha = 20$ deg.

obtained. The pressure distributions shown in Fig. 3 were obtained from a converged steady-state solution within 30–50 time steps. As shown, with no wakes, the potential flow predicts a high suction at the base corner, in particular at the windward side surface, $\theta = 0$ deg, as expected. The wake introduced at the base corner reduces the suction significantly. However, it is observed that the larger the time step, the smaller the reduction on the surface pressure distribution. The magnitude of the time step sets the size of the wake panels. The larger reduction due to small time-step size, therefore, is attributed to the proximity of the wake panels to the corner region, which gets smaller with smaller time steps. The wake panels closer to the body have a stronger influence on the corner flow. Yet time steps smaller than 0.2 did not produce converged solutions along the time steps, which we attributed to a possible instability due to the very close proximity of the wake panels to the surface panels. In the rest of the computations, we used a fixed time-step size of $\Delta t = 0.3$.

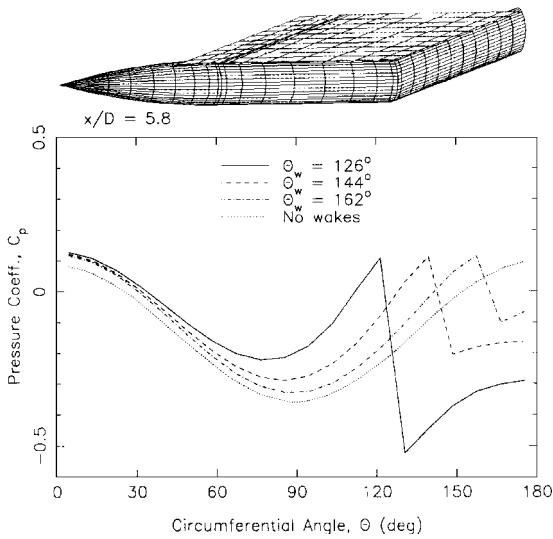


Fig. 4 Influence of circumferential position of body wake separation line on surface pressure distribution at $\alpha = 20$ deg.

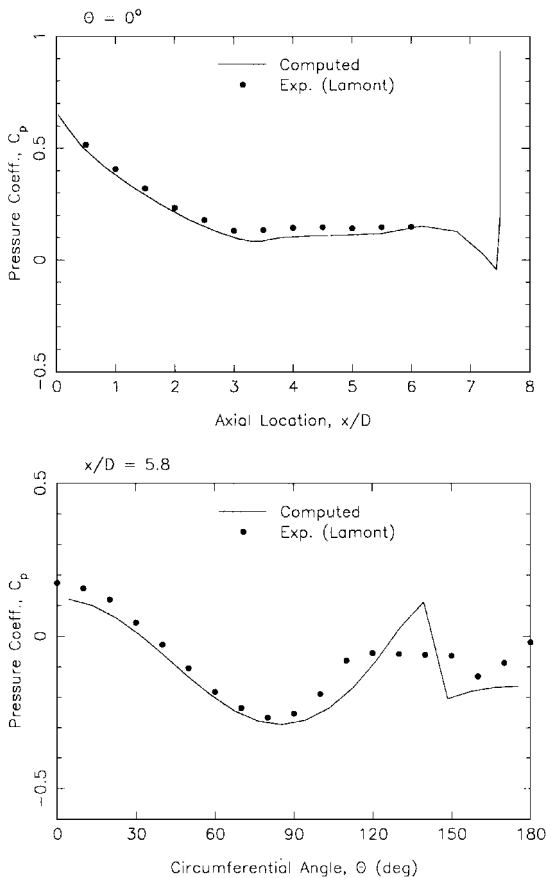


Fig. 5 Surface pressure distribution at $\alpha = 20$ deg, $\Theta_w = 144$ deg.

Next, in addition to the vortex wake shed from the base corner, another wake along the ogive cylinder body at a prescribed circumferential position Θ_w was introduced to model the flow separation over the body. The axial locations of the wake separation lines from the body were fixed at $3.0D$ – $7.5D$. The circumferential position was varied at $\Theta_w = 126$ – 162 deg. As shown in Fig. 4, the pressure distribution in the circumferential direction is a strong function of the circumferential position of the wake separation line. At the wake separation line, the potential flow solution assumes a stagnation-type flow and predicts relatively high pressure. However, past the wake separation line a strong suction pressure, which is induced by the wake panels, is observed. As the wake separation line comes closer to $\Theta_w = 90$ deg, the induced suction increases significantly. This behavior again is attributed to the closer proximity of

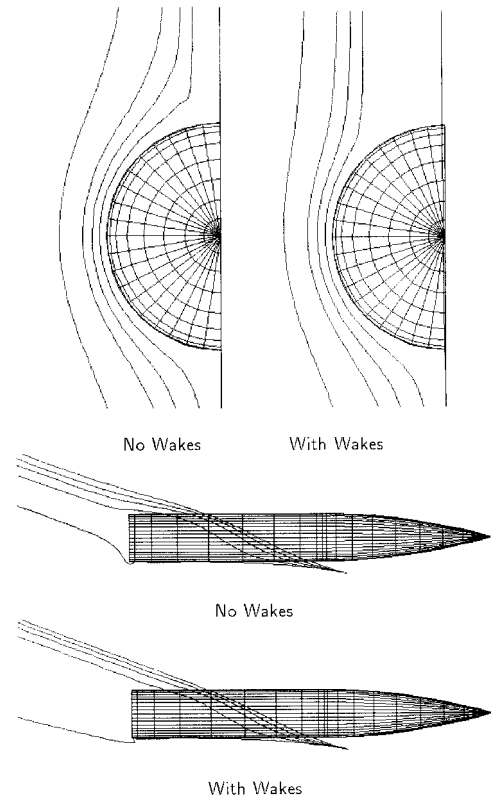


Fig. 6 Offbody streamlines at $\alpha = 20$ deg.

the nascent wake panels to the surface as they are placed more and more tangent to the surface.

In Fig. 5, the computed surface pressure distributions with $\Theta_w = 144$ deg are compared against the experimental data by Lamont.^{15,16} However, we extracted the experimental data from Ref. 4. The experimental data are reported to be obtained at $\alpha = 20$ deg, $Re_D = 4 \times 10^6$, and $M_\infty \leq 0.3$. In the experiment of Refs. 15 and 16, the last axial station at which the measurements were taken is at $x/D = 6.0$. It is reported¹⁶ that for fully turbulent flow the separation line is located at about $\Theta = 105$ – 110 deg. At the windward side, $\Theta = 0$ deg, the potential flow solution agrees well with the experimental data. At $x/D = 5.8$, good agreement is obtained up to the flow separation line. At the wake separation line, the potential flow overpredicts the surface pressure by as much as $\Delta C_p = 0.16$, whereas on the leeward side, past the wake separation line, the pressure is slightly underpredicted. Figure 6 shows the computed offbody streamlines with wakes and no wakes. The graphical post-processing of the computed offbody streamlines was done using POSTMARC software¹⁷ running on PC Windows. Although vortical structures and a possible vortex rollup on the leeward side of the body may not be predicted, it is clearly observed that the body and the base corner wakes simulate the flow separation to a certain extent. The flow with wakes does not experience the symmetric flow behavior in the crossflow plane, and the strong influence of high base corner suction in the case of no wakes is not observed anymore.

Figure 7 shows the circumferential pressure distribution at $\alpha = 15$ deg for two axial locations, $x/D = 1.5$ and 5.0 . The body wake similarly starts from $x/D = 3.0$ and is shed from the $\Theta_w = 144$ deg circumferential position. The computed pressure distributions again agree well with the experimental data^{15,16} (extracted from Ref. 7) at locations before and after the wake separation line.

Next we computed the flowfield at $\alpha = 30$ deg. The windward-side axial pressure distribution and the circumferential pressure distribution with various body wake separation line locations are shown in Fig. 8. Although the computed pressure values agree well with the experimental data^{15,16} (extracted from Ref. 4) on the windward side, they are substantially overpredicted at the base corner and the separated-flow region. Therefore, it is concluded that the simulation of flow separation using rigid wakes fails to predict the flowfield within an acceptable accuracy at high incidences.

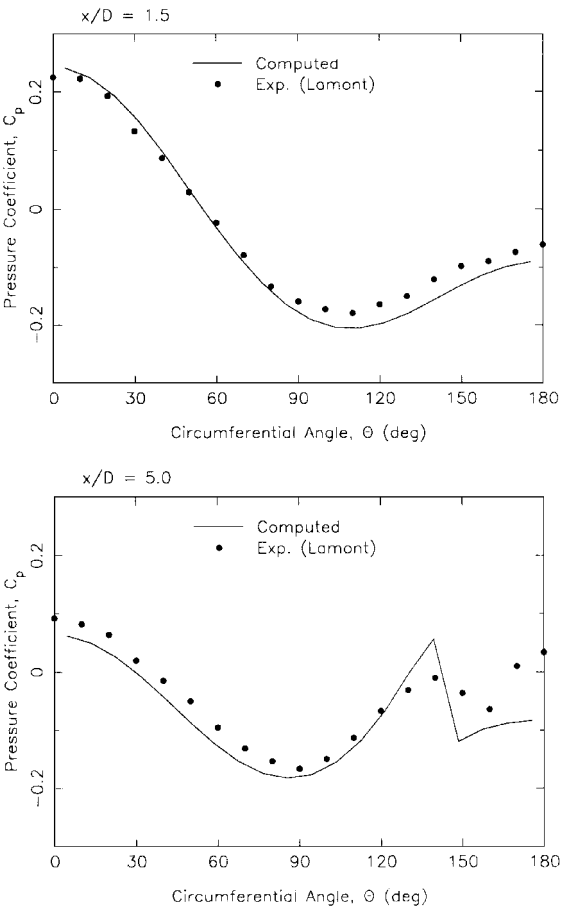


Fig. 7 Surface pressure distribution at $\alpha = 15$ deg, $\Theta_w = 144$ deg.

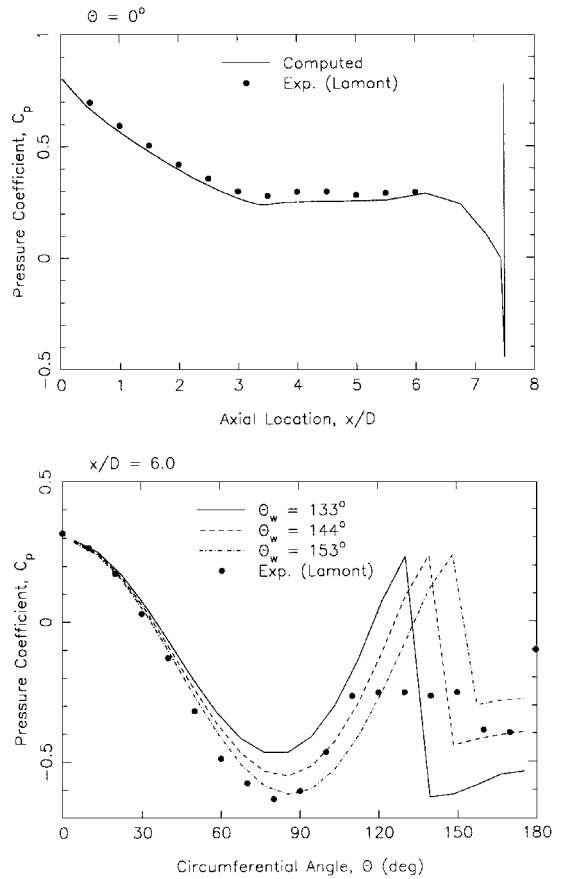


Fig. 8 Surface pressure distribution at $\alpha = 30$ deg.

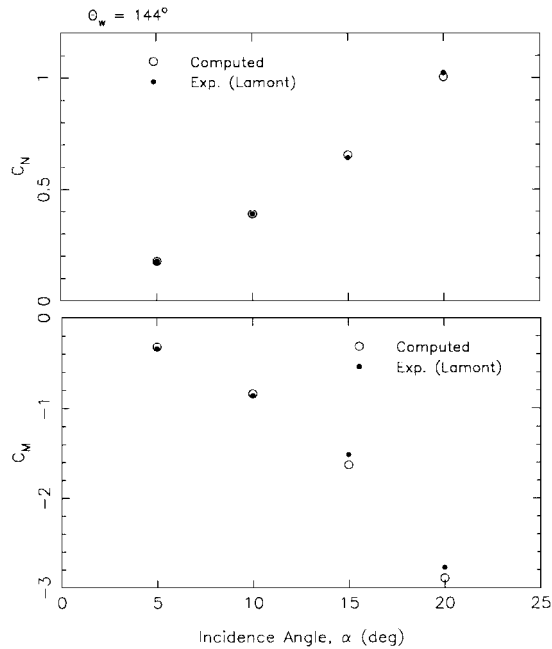


Fig. 9 Normal force and pitching-moment coefficients.

The normal force and pitching-moment coefficients are given in Fig. 9. The same model with body and base corner wakes was used for the low-incidence computations, and the base contribution is included in the aerodynamic force calculations. As shown, the computed aerodynamic forces are in good agreement with the experimental data^{15,16} (extracted from Ref. 7). It appears that at low incidences the high- and the low-pressure peaks at the wake separation line cancel each other for a better representation of the integrated forces in the separated-flow region. However, notice that, at high incidences, the normal force and pitching moment are predicted to be slightly lower than the experimental data, which may be attributed to the low pressure induced at the base corner and to the high pressure at the wake separation line on the body.

Concluding Remarks

The PMARC potential flow solver was employed to compute subsonic flowfields over an ogive cylinder body. Rigid wakes were introduced at the base corner and along the cylindrical body to simulate flow separation. The computed surface pressure distributions and the total normal force and pitching-moment coefficients agree well with the experimental data up to about 20-deg incidence. It is concluded that PMARC may be employed as a computationally efficient tool in aerodynamic missile design work for the 0- to 20-deg incidence range. Further investigations are required to explore the higher incidence range with flexible and asymmetric wakes.

Acknowledgments

The authors wish to thank David Siegel, Office of Naval Research, and Craig Porter and C. Housh, U.S. Naval Air Warfare Center, Weapons Division, China Lake, California, for their support of this project.

References

¹Mendenhall, R. M. (ed.), *Tactical Missile Aerodynamics: Prediction Methodology*, 2nd ed., Vol. 142, Progress in Astronautics and Aeronautics, AIAA, Washington, DC, 1992.

²Rom, J., *High Angle of Attack Aerodynamics*, Springer-Verlag, New York, 1992, pp. 78–384.

³Moore, F. G., McInville, R. M., and Hymer, T. C., “The 1995 Version of the NSWC Aeroprediction Code, Part 1: Summary of New Theoretical Methodology,” U.S. Naval Surface Warfare Center, Dahlgren Div., TR-94/379, Dahlgren, VA, Feb. 1995.

⁴Degani, D., Schiff, L. B., and Levy, Y., “Physical Considerations Governing Computation of Turbulent Flows over Bodies at Large Incidence,” AIAA Paper 90-0096, Jan. 1990.

⁵Vatsa, V. N., Thomas, J. L., and Wedan, B. W., "Navier-Stokes Computations of Prolate Spheroids at Angle of Attack," AIAA Paper 87-2627, Aug. 1987.

⁶Ying, S. X., Schiff, L. B., and Steger, J. L., "A Numerical Study of Three-Dimensional Separated Flow Past a Hemisphere Cylinder," AIAA Paper 87-1207, June 1987.

⁷Almosnino, D., "High Angle-of-Attack Calculations of the Subsonic Vortex Flow on Slender Bodies," *AIAA Journal*, Vol. 28, No. 8, 1985, pp. 1150-1156.

⁸Almosnino, D., and Rom, J., "Calculation of Symmetric Vortex Separation Affecting Subsonic Bodies at High Incidence," *AIAA Journal*, Vol. 21, No. 3, 1983, pp. 398-406.

⁹Ekaterinaris, J. A., "Analysis of Flowfields over Missile Configurations at Subsonic Speeds," *Journal of Spacecraft and Rockets*, Vol. 32, No. 3, 1995, pp. 385-391.

¹⁰Hsieh, T., Priolo, F. J., Wardlaw, A. B., Jr., and VanDyken, R. D., "Navier-Stokes Calculation of Flow over a Complete Missile to 60 Degree Incidence," AIAA Paper 95-0760, Jan. 1995.

¹¹Tuncer, I. H., Platzer, M. F., and VanDyken, R. D., "A Computational Study of Subsonic Flowfields over a Missile Configuration," AIAA Paper 97-0635, Jan. 1997.

¹²Lambert, M. A., and Platzer, M. F., "Evaluation of the NASA-Ames Panel Method (PMARC) for Aerodynamic Missile Design," AIAA Paper 96-0775, Jan. 1996.

¹³Tuncer, I. H., Marvin, R., and Platzer, M. F., "Numerical Investigation of Subsonic Flow over a Typical Missile Forebody," AIAA Paper 96-0189, Jan. 1996.

¹⁴Ashby, D. L., Dudley, M. R., Iguchi, S. K., Browne, L., and Katz, J., "Potential Flow Theory and Operational Guide for the Panel Code PMARC-12," COSMIC Program ARC-13362, COSMIC, Athens, GA, Dec. 1992.

¹⁵Lamont, P. J., "Pressure Around an Inclined Ogive Cylinder with Laminar, Transitional, or Turbulent Separation," *AIAA Journal*, Vol. 20, No. 11, 1982, pp. 1482-1499.

¹⁶Lamont, P. J., "The Complex Asymmetric Flow over a 3.5D Ogive Nose and Cylindrical Afterbody at High Angles of Attack," AIAA Paper 82-0053, Jan. 1982.

¹⁷Pinella, D., "POSTMARC, A Windows Postprocessor for CMARC and PMARC-12," Personal Simulation Works, Aerologic, Los Angeles, CA, June 1996.

R. M. Cummings
Associate Editor